Proceedings of the 7th International Conference on HydroScience and Engineering

Philadelphia, USA September 10-13, 2006 (ICHE 2006)

ISBN: 0977447405

Drexel University

College of Engineering

THREE-DIMENSIONAL SHAPE IDENTIFICATION OF BODY LOCATED IN VISCOUS FLUID FLOW

Kazuya Nojima [1] **and Mutsuto Kawahara** [2]

ABSTRACT

This paper presents a numerical method of shape identification of a body located in incompressible viscous flow. The purpose of this research is to identify the optimal shape that minimizes the fluid forces subjected to the body. The formulation of the shape identification is based on the optimal control theory. The finite element method is used for calculation of fluid flow.
In this paper, optimal control is treated as fluid force minimization. The first thing that should be carried out in the optimal control theory is to define a performance function which expresses the optimal shape. The performance function must be minimized satisfying the state equation. In the research, the Lagrange multipliers are introduced for the constraint conditions.
To avoid the break down of calculation caused by destruction of elements, the finite element mesh is reconstructed in the identification process. The grid generation scheme based on Delaunay triangulation is applied to the reconstruction of finite element mesh. The Delaunay triangulation is expanded to three dimensions.
In this paper, an optimized shape of the body is obtained by computation. The final shape is compared with the shape obtained by O. Pironneau.

Keywords: Finite element method, Shape identification, Optimal control theory, Tree-dimensional mesh generation, Delaunay tetrahedrization

1 INTRODUCTION

It is well known that the shape of the body in incompressible viscous flow field which has the minimum drag force is the streamline configuration. These are suggested by only experiments and the numerical computations are not sufficiently carried out about this problem. The purpose of this study is to determine an drag minimum shape of the body located in an incompressible viscous flow applying a formulation of the shape identification to a numerical simulation.

The formulation of the shape identification is based on the optimal control theory, see Matsumoto (2002) and Ogawa (2003). The finite element method is used for calculation of fluid flow. The first thing that should be carried out in the optimal control theory is to define a performance function which expresses the drag minimum shape. The performance function must

[1]Ph.D. Student, Department of Civil Engineering, Chuo University Kasuga 1-13-27, Bunkyo-ku, Tokyo 112-8551, Japan (noji@kc.chuo-u.ac.jp)

[2]Professor, Department of Civil Engineering, Chuo University Kasuga 1-13-27, Bunkyo-ku, Tokyo 112-8551, Japan (kawa@civil.chuo-u.ac.jp)

be minimized satisfying the state equation. Thus the minimization problem with constraint condition is required. In the research, the Lagrange multipliers are introduced. Although then shape identification problem is the minimization problem with constraint condition, it can be transformed into the minimization problem without constraint condition using the Lagrange multiplier method. The performance function based on the Lagrange multipliers is called the extended performance function. The stationary condition is that the first variation of the extended performance function is equal to zero.
The shape is renewed by a minimization technique. The gradient based method is used in this research.

There are some problems. One of them is breaking down of the finite element mesh. The shape of the body is changed in identification process. The finite element mesh, also, should be changed. In previous research, finite element mesh is renewed by moving nodal points. However, process of moving nodal points causes of generating negative volume or zero volume elements. These elements are unlike to obtain accurate solution. The calculation will be stopped when the destruction of elements occurs. To avoid the break down of calculation caused by destruction of elements, the finite element mesh is reconstructed in identification process. The grid generation scheme based on Delaunay triangulation is applied to the reconstruction of finite element mesh. The Delaunay triangulation is expanded to three dimensions.

In this paper, an optimized shape of the body is obtained by computation. In the optimizing computation, a sphere is set in the computational domain as initial shape of the body. The final shape is compared with the shape obtained by O. Pironneau (1973 and 1974). Pironneau proposed the method of changing shape optimally using the gradient which is determined by taking variation with respect to coordinate. A good agreement is observed between the result obtained in this research and the result obtained by O. Pironneau.

2 GOVERNING EQUATION

2.1 Navier-Stokes Equation

Consider a typical problem described in figure 1, in which a solid body B with the boundary Γ_B, is laid in an external flow. Let Γ denote the boundary of Ω, suppose that an incompressible viscous flow occupies Ω. The state equation of the flow can be written by the Navier-Stokes equation in the non-dimensional form,

$$\dot{u_i} + u_j u_{i,j} + p_{,i} - \nu(u_{i,j} + u_{j,i})_{,j} = 0 \qquad in \qquad \Omega, \tag{1}$$

$$u_{i,i} = 0 \qquad in \qquad \Omega, \tag{2}$$

where u_i, p and ν are the velocity, pressure, and the viscosity coefficient , respectively. Suppose that the boundary conditions are given as follows;

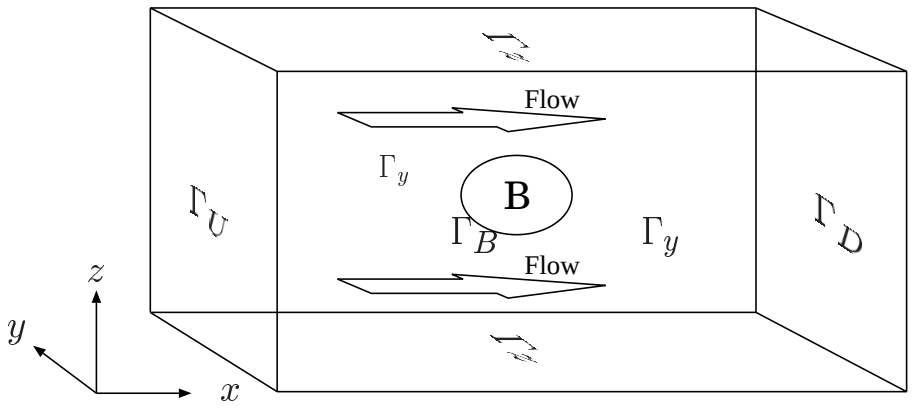

Figure 1: Computational domain and boundary condition

$$u_i = \hat{u}_i \quad on \quad \Gamma_U, \tag{3}$$

$$t_1 = 0, \quad u_2 = 0 \quad on \quad \Gamma_y, \tag{4}$$

$$t_1 = 0, \quad u_3 = 0 \quad on \quad \Gamma_z, \tag{5}$$

$$u_i = 0 \quad on \quad \Gamma_B, \tag{6}$$

$$t_i = 0 \quad on \quad \Gamma_D, \tag{7}$$

where

$$t_i = \{-p\delta_{ij} + \nu(u_{i,j} + u_{j,i})\}n_j, \tag{8}$$

in which t_i is traction, and n_j is a unit outward normal to the boundary Γ, respectively. δ_{ij} is Kronecker's δ.

The fluid forces subjected to the body are denoted by F_i, where F_1, F_2 and F_3 are drag, side and lift forces, respectively. The fluid force F_i is obtained by integrating the traction t_i on the boundary, Γ_B as,

$$F_i = -\int_{\Gamma_B} t_i d\Gamma. \tag{9}$$

2.2 Discretization – Mixed interpolation

The weighted residual equation of the basic equation is written as follows;

$$\int_\Omega w_i \dot{u}_i d\Omega + \int_\Omega w_i u_j u_{i,j} d\Omega + \int_\Omega w_{i,j}\{-p\delta_{ij} + \nu(u_{i,j} + u_{j,i})\}d\Omega = \int_\Gamma w_i t_i d\Gamma, \tag{10}$$

$$\int_\Omega q u_{i,i} d\Omega = 0, \tag{11}$$

As the spatial discretization, the finite element method using mixed interpolation method presented by Matsumoto (1999 and 2000) is applied for the state equation. The mixed interpolation for the momentum and pressure equations can be expressed, which is

a) bubble function interpolation for velocity

$$u_i = \Phi_1 u_{i1} + \Phi_2 u_{i2} + \Phi_3 u_{i3} + \Phi_4 u_{i4} + \Phi_5 \tilde{u}_{i5}, \tag{12}$$
$$\tilde{u}_{i5} = u_{i5} - \frac{1}{4}(u_{i1} + u_{i2} + u_{i3} + u_{i4}),$$

$$w_i = \Phi_1 w_{i1} + \Phi_2 w_{i2} + \Phi_3 w_{i3} + \Phi_4 w_{i4} + \Phi_5 \tilde{w}_{i5}, \tag{13}$$
$$\tilde{w}_{i5} = w_{i5} - \frac{1}{4}(w_{i1} + w_{i2} + w_{i3} + w_{i4}),$$

$$\Phi_1 = \eta_1, \quad \Phi_2 = \eta_2, \quad \Phi_3 = \eta_3, \quad \Phi_4 = \eta_4, \quad \Phi_5 = 256\eta_1\eta_2\eta_3\eta_4,$$

and

b) linear interpolation for pressure

$$p = \Psi_1 p_1 + \Psi_2 p_2 + \Psi_3 p_3 + \Psi_4 p_4, \tag{14}$$

$$q = \Psi_1 q_1 + \Psi_2 q_2 + \Psi_3 q_3 + \Psi_4 q_4, \tag{15}$$

$$\Psi_1 = \eta_1, \quad \Psi_2 = \eta_2, \quad \Psi_3 = \eta_3, \quad \Psi_4 = \eta_4,$$

where Φ_α (α = 1,5) is the bubble function in five-node tetrahedral element, Ψ_λ (λ = 1,4) is the linear interpolation for pressure in four-node tetrahedral element and $u_{i\alpha}$ and p_λ represent the nodal values at the α^{th} node of each finite element, respectively.

The criteria for the steady problem is used, in which the discretized form derived by the bubble function interpolation is equivalent to those by the SUPG method, presented by Hughes (1986). In the bubble function element for the steady problem, the stabilized parameter τ_{eB} which determines the magnitude of the streamline stabilized term can be given by;

$$\tau_{eB} = \frac{< \phi_e, 1 >^2_{\Omega_e}}{(\nu + \nu')\|\phi_{e,j}\|^2_{\Omega_e} A_e}, \tag{16}$$

where $< u', v' >_{\Omega_e} = \int_{\Omega_e} u'v' d\Omega$, $\|u'\|^2_{\Omega_e} = \int_{\Omega_e} u'u' d\Omega$ and $A_e = \int_{\Omega_e} d\Omega$. From the criteria for the stabilized parameter in the SUPG method, an optimal parameter τ_{eS} can be chosen as;

$$\tau_{eS} = \left[\left(\frac{2|u_i'|}{h_e} \right)^2 + \left(\frac{4\nu}{h_e^2} \right)^2 \right]^{-\frac{1}{2}}, \tag{17}$$

where h_e is an element size.
Generally, Eq. (16) is not equal to Eq. (17). The bubble function that gives optimal viscosity satisfies the following equation expressed by the stabilized operator control parameter ν;

$$\frac{< \phi_e, 1 >^2_{\Omega_e}}{(\nu + \nu')\|\phi_{e,j}\|^2_{\Omega_e} A_e} = \tau_{eS}, \tag{18}$$

It is shown that Eq. (18) adds stabilized operator control term (19) only of the barycenter point to the equation of motion;

$$\sum_{e=1}^{N_e} \nu' \|\phi_{e,j}\|^2_{\Omega_e} b_e, \tag{19}$$

where N_e and b_e are the total number of elements and barycenter point.

2.3 Finite element equation

The finite element equation can be described as follows,

$$\mathbf{M}\dot{\mathtt{u}}_i + \mathbf{A}_{,j}(\mathtt{u}_j)\mathtt{u}_i - \mathbf{C}_{,i}\mathtt{p} + \mathbf{D}_{,jj}\mathtt{u}_i + \mathbf{D}_{,ji}\mathtt{u}_j = T_i \qquad in \qquad \Omega, \tag{20}$$

$$\mathbf{C}_{,i}{}^T\mathtt{u}_i = 0 \qquad in \qquad \Omega, \tag{21}$$

where,

$$\mathbf{M} = \sum^{N_e} \int_{\Omega_e} \Phi_\alpha \Phi_\beta d\Omega, \ \mathbf{D}_{,ji} = \sum^{N_e} \nu \int_{\Omega_e} \Phi_{\alpha,j} \Phi_{\beta,i} d\Omega, \ \mathbf{A}_{,i}(\mathtt{u}_i) = \sum^{N_e} \int_{\Omega_e} \Phi_\alpha \Phi_\gamma \mathtt{u}_{i\gamma} \Phi_{\beta,i} d\Omega,$$
$$(\alpha = 1, \cdots, 5 \quad \beta = 1, \cdots, 5 \quad \gamma = 1, \cdots, 5)$$
$$\mathbf{C}_{,i} = \sum^{N_e} \int_{\Omega_e} \Psi_{\alpha,i} \Psi_\beta d\Omega,$$
$$(\alpha = 1, \cdots, 5, \quad \beta = 1, \cdots, 4)$$
$$T_i = \sum^{N_s} \int_{\Gamma_B} \eta_\alpha t_i d\Gamma,$$
$$(\alpha = 1, 2, 3)$$

The function η are the interpolation function for each element of boundary. The approximated trial function of the velocity and pressure are denoted by $\mathtt{u}_i$, $\mathtt{p}$, respectively.

3 SHAPE DETERMINATION

In this research, applying the shape determination algorithm, the shape which minimized fluid forces subjected to the body under the constraints of the Navier-Stokes equations. Coordinate of boundary of the shape is applied to design parameter of shape determination $\mathtt{x}_i$.

3.1 Volume constraint

The shape of the body should be optimized keeping the volume constant. The volume is being kept in each iteration cycle. To keep the volume of the body is equal to keep the volume of the whole computational domain. The volume constraint function yields as follows,

$$\sum_{e=1}^{m} a_e(\mathtt{x}_i) - A_0 = 0, \tag{22}$$

where $a_e(\mathtt{x}_i)$ is the volume of each element and A_0 is the volume of the initial analytical domain.

3.2 Performance function

In this paper, a fluid force control problem is treated. The performance function J is defined by the square sum of the residual between values of computed fluid force and objective fluid force, as Maruoka (1998) shows,

$$J = \frac{1}{2}\int_{t_0}^{t_f} (q_1 F_1^2 + q_2 F_2^2 + q_3 F_3^2) dt, \tag{23}$$

q_1, q_2 and q_3 are the weighting parameter of the drag, lift and side forces, respectively. The performance function should be minimized satisfying Eqs. (20) and (21). The Lagrange multiplier method is suitable for the optimal control problem with the constraint conditions. The Lagrange multipliers for Eqs. (20) and (21) and volume constraint are defined as adjoint velocity $\mathtt{u}_i^*$ and pressure $\mathtt{p}^*$ and λ. This problem can be transformed into the stationary problem of the extended performance function J^* which can be obtained by adding the dot product between adjoint velocity $\mathtt{u}_i^*$, pressure $\mathtt{p}^*$ and Lagrange multiplier of volume constraint function λ and Eqs. (20) and (21) to original performance function as follows,

$$\begin{aligned} J^* &= \frac{1}{2}\int_{t_0}^{t_f} (q_1 F_1^2 + q_2 F_2^2 + q_3 F_3^2) dt \\ &\quad - \int_{t_0}^{t_f} \mathtt{u}_i^{*T}(\mathbf{M}\dot{\mathtt{u}}_i + \mathbf{A}_{,j}(\mathtt{u}_j)\mathtt{u}_i - \mathbf{C}_{,i}\mathtt{p} + \mathbf{D}_{,jj}\mathtt{u}_i + \mathbf{D}_{,ji}\mathtt{u}_j - T_i) dt \\ &\quad + \int_{t_0}^{t_f} \mathtt{p}^{*T}\mathbf{C}_{,i}{}^{T}\mathtt{u}_i dt \\ &\quad + \mathtt{a}^*\{\sum_{e=1}^{m} a_e(\mathtt{x}_i) - A_0\}, \end{aligned} \tag{24}$$

where, discretized velocity and pressure are denoted by $\mathtt{u}_i$ and $\mathtt{p}$, respectively.

3.3 Stationary condition

The optimal control problem with the constraint condition of Eqs. (20) and (21) results in solving a stationary condition of the extended performance function J^* instead of the original performance function J. The stationary condition is $\delta J^* = 0$. The first variation of the extended performance function J^* can be derived as follows;

$$
\begin{aligned}
\delta J^* \;=\; & -\int_{t_0}^{t_f} \delta \mathtt{u}_i^{*T}(\mathbf{M}\dot{\mathtt{u}}_i + \mathbf{A}_{,j}(\mathtt{u}_j)\mathtt{u}_i - \mathbf{C}_{,i}\mathtt{p} + \mathbf{D}_{,jj}\mathtt{u}_i + \mathbf{D}_{,ji}\mathtt{u}_j - T_i)dt \\
& + \int_{t_0}^{t_f} \delta \mathtt{p}^{*T}\mathbf{C}_{,i}{}^T\mathtt{u}_i dt \\
& - \int_{t_0}^{t_f} \delta \mathtt{u}_i{}^T(-\mathbf{M}\dot{\mathtt{u}}_i^* + \mathbf{A}_{,j}{}^T(\mathtt{u}_j)\mathtt{u}_i^* - \mathbf{C}_{,i}\mathtt{p}^* + \mathbf{D}_{,jj}{}^T\mathtt{u}_i^* + \mathbf{D}_{,ij}{}^T\mathtt{u}_j^*)dt \\
& + \int_{t_0}^{t_f} \delta \mathtt{p}^T\mathbf{C}_{,i}{}^T\mathtt{u}_i^* dt \\
& + \int_{t_0}^{t_f} \delta T_i{}^T(\mathtt{u}_i^* - q_i F_i)dt \\
& + \delta \mathtt{a}^{*T}\{\sum_{e=1}^{m} a_e(\mathtt{x}_i) - A_0\} \\
& + \delta \mathtt{x}_i{}^T G_i, \qquad (25)
\end{aligned}
$$

where

$$
\begin{aligned}
G_k \;=\; & \frac{\partial J^*}{\partial \mathtt{x}_k} \\
=\; & -\int_{t_0}^{t_f} \mathtt{u}_i^{*T}(\frac{\partial \mathbf{M}}{\partial \mathtt{x}_k}\dot{\mathtt{u}}_i + \frac{\partial \mathbf{A}_{,j}(\mathtt{u}_j)}{\partial \mathtt{x}_k}\mathtt{u}_i - \frac{\partial \mathbf{C}_{,i}}{\partial \mathtt{x}_k}\mathtt{p} + \frac{\partial \mathbf{D}_{,jj}}{\partial \mathtt{x}_k}\mathtt{u}_i + \frac{\partial \mathbf{D}_{,ji}}{\partial \mathtt{x}_k}\mathtt{u}_j - \frac{\partial T_i}{\partial \mathtt{x}_k})dt \\
+\; & \int_{t_0}^{t_f} \mathtt{p}^{*T}\frac{\partial \mathbf{C}_{,i}{}^T}{\partial \mathtt{x}_k}\mathtt{u}_i dt + \mathtt{a}^{*T}\frac{\partial}{\partial \mathtt{x}_k}\sum_{e=1}^{m} a_e(\mathtt{x}_i), \qquad (26)
\end{aligned}
$$

in which G_k gives the gradient of the extended performance function and $\mathtt{x}_i$ is the coordinate around the body. Setting each term equal to zero to satisfy the optimal condition, the following conditions are required.

$$\mathbf{M}\dot{\mathtt{u}}_i + \mathbf{A}_{,j}(\mathtt{u}_j)\mathtt{u}_i - \mathbf{C}_{,i}\mathtt{p} + \mathbf{D}_{,jj}\mathtt{u}_i + \mathbf{D}_{,ji}\mathtt{u}_j = T_i \quad in \quad \Omega, \tag{27}$$

$$\mathbf{C}_{,i}{}^T\mathtt{u}_i = 0 \quad in \quad \Omega, \tag{28}$$

$$\mathbf{M}^T\dot{\mathtt{u}}_i^* + \mathbf{A}_{,j}{}^T(\mathtt{u}_j)\mathtt{u}_i^* - \mathbf{C}_{,i}\mathtt{p}^* + \mathbf{D}_{,jj}{}^T\mathtt{u}_i^* + \mathbf{D}_{,ji}{}^T\mathtt{u}_j^* = 0 \quad in \quad \Omega, \tag{29}$$

$$\mathbf{C}_{,i}{}^T\mathtt{u}_i^* = 0 \quad in \quad \Omega, \tag{30}$$

$$q_i F_i - \mathtt{u}_i^* = 0 \quad on \quad \Gamma_B, \tag{31}$$

$$\sum_{e=1}^{m} a_e(\mathtt{x}_i) - A_0 = 0 \quad in \quad \Omega, \tag{32}$$

$$G_i = 0 \quad in \quad \Omega, \tag{33}$$

if $\mathtt{u}_i$, $\mathtt{p}$, $\mathtt{u}_i^*$ and $\mathtt{p}^*$ are solved satisfying Eqs. (27) to (31), the first variation of the extended performance function J^* can be rewritten as follows;

$$\delta J^* = \delta\mathtt{x}_i{}^T G_i. \tag{34}$$

The optimal condition of this problem is given by

$$\frac{\partial J^*}{\partial \mathtt{x}_i} = G_i = 0. \tag{35}$$

4 MINIMIZATION TECHNIQUE

As the minimization technique, the gradient based method is applied in this paper. In this method, a modified performance function K, which can be obtained by adding a penalty term to the extended performance function, is introduced. The modified performance function is

$$K^{(l)} = J^{*(l)} + \frac{1}{2}\left(\mathtt{x}_i^{(l+1)} - \mathtt{x}_i^{(l)}\right)^T Q\left(\mathtt{x}_i^{(l+1)} - \mathtt{x}_i^{(l)}\right), \tag{36}$$

where l is the iteration number for minimization. $\mathtt{x}_i$ and Q are the coordinate of the body and weighting diagonal matrix, respectively. If the modified performance function K converged to the minimum, the penalty term will be zero. To minimize the modified performance function K is equal to minimizing the extended performance function J^*.
Let $\mathtt{x}_i$ be the optimal solution of the coordinate, then the following equality should hold,

$$\delta K^{(l)} = 0. \tag{37}$$

the first variation of the modified performance function δK, can be written as follows;

$$\delta K^{(l)} = \delta J^* + \delta\mathtt{x_i}{}^T Q\left(\mathtt{x}_i^{(l+1)} - \mathtt{x}_i^{(l)}\right). \tag{38}$$

Thus, Eq.(26), (34) and (37) gives

$$G_i + Q\left(\mathtt{x}_i^{(l+1)} - \mathtt{x}_i^{(l)}\right) = 0, \tag{39}$$

and the renewed surface coordinates of the body is calculated at each iteration by the following equation,

$$\mathtt{x}_i^{(l+1)}\Big|_{\Gamma_B} = \mathtt{x}_i^{(l)}\Big|_{\Gamma_B} - Q^{-1}\, G_i^{(l)}\Big|_{\Gamma_B}. \tag{40}$$

4.1 Algorithm

The following algorithm can be introduced.

1. Set iteration number $l = 0$.
2. Select initial surface coordinates $\mathtt{x}_i{}^{(0)}$ in Ω.
3. Solve $\mathtt{u}_i{}^{(0)}$, $\mathtt{p}^{(0)}$ by Eqs. (27) and (28) in Ω.
4. Compute $J^{(0)}$.
5. Solve $\mathtt{u}_i^{*(0)}$, $\mathtt{p}^{*(0)}$ by Eqs. (29), (30) and (31) in Ω.
6. Set $l = l + 1$.
7. Compute $\mathtt{x}_i{}^{(l)}$ by Eq. (40).
8. If $\left|\mathtt{x}_i{}^{(l)} - \mathtt{x}_i{}^{(l-1)}\right| < \varepsilon$ then stop.
9. Update computational domain and finite element mesh.
10. Solve $\mathtt{u}_i{}^{(l)}$, $\mathtt{p}^{(l)}$ by Eqs.(27) and (28) in Ω.
11. Compute $J^{(l)}$.
12. Solve $\mathtt{u}_i^{*(l)}$, $\mathtt{p}^{*(l)}$ by Eqs. (29), (30) and (31), go to 6.

5 FINITE ELEMENT MESH GENERATION

5.1 The Delaunay Triangulation

Dirichlet in 1850, first proposed a method whereby a domain could be systematically decomposed into a set of packed convex polyhedra. For a given set of points in space, $\{P_k\}, k = 1, \cdots, K$, the regions$\{V_k\}, k = 1, \cdots, K$, are the territories which can be assigned to each point P_k, such that V_k represents the space closer to P_k than to any other point in the set. Clearly, these regions satisfy

$$V_k = \{P_i : |p - P_i| < |p - Pj|, \forall j \neq i\}\,. \tag{41}$$

This geometrical construction of tiles is known as the Dirichlet tessellation or Voronoi diagram. This tessellation of a closed domain results in a set of non-overlapping convex polyhedra, called Voronoi regions, covering the entire domain. If all point pairs which have some segment of a Voronoi boundary in common are joined, the result is a triangulation of the convex bull of the set of points $\{P_k\}$. This triangulation is known as the Delaunay triangulation. The definition is valid for n-dimensional space.

From the above discussion, it is apparent that in two dimensions a line segment of the Voronoi diagram is equidistant from the two points it separates. Hence, the vertices of the Voronoi diagram must be equidistant from each of the three nodes which form the Delaunay triangles.

Clearly, it is possible to construct a circle, centered at a Voronoi vertex, which passed through the three points which form a triangle. Furthermore, it is evident that, given the definition of Voronoi line segments and regions, no circle can contain any point. This latter condition is referred to as the in-circle criterion.

These observation are also true for n-dimensional space. Hence, in three dimensions a vertex of a Voronoi diagram is at the center of circumscribed sphere which passes through four points which form a tetrahedron and no other point in the construction can lie within the sphere.

The Delaunay triangulation and its geometrical properties have been widely known for a considerable time. However, the application of the construction to mesh generation technique has only relatively recently been explored.

In general, the use of the Delaunay triangulation for grid generation requires a set of points interior to a given domain. Unfortunately, the Delaunay criterion does not give any indication as to how points should be defined. It is necessary, therefore, to construct a way of grid point generation for arbitrary geometries.

5.2 The Delaunay Algorithm

The algorithm used to generate the Delaunay triangulation follows the same steps as for the two-dimensional construction and is based upon the work of Bowyer (1981). The Delaunay algorithm of Bowyer, which is based on the in-circle criterion, is a sequential process; each point is introduced into an existing Delaunay satisfying structure, which is broken and then reconnected to form a new Delaunay triangulation.

In three dimensions the algorithm, in step-by-step format is as follows.

Algorithm

1. Define a set of points which form a convex hull within which all points will lie. An appropriate Delaunay data structure is established for this construction. It should be noted that some vertices of the associated Voronoi diagram are not strictly defined, since they lie outside the convex hull and therefore do not possess four forming points of the tetrahedron and do not have four neighbor Voronoi vertices.

2. Introduce a new point anywhere within convex hull.

3. Determine all vertices of the Voronoi diagram to be deleted. A point which lies within a sphere, centered at a vertex of the Voronoi diagram and which passes through its four forming points, results in the deletion of the vertex. This follows from the 'in-circle' criterion of the Voronoi construction.

4. Find the forming points of all the deleted Voronoi vertices. These are the contiguous points to the new point.

5. Determine the neighboring Voronoi vertices to the deleted vertices which have not themselves been deleted. These data provide the necessary information to enable valid combination of the contiguous points to be constructed.

6. Determine the forming points of the new Voronoi vertices. The forming points of new vertices must include the new point together with three points which are contiguous to the new point and form a face of a neighboring tetrahedra.

7. Determine the neighboring Voronoi vertices to the new Voronoi vertices as found in Step 5, to identify common triples of forming points. When a common combination occurs, neighbor of the Voronoi diagram have been found.

8. Reorder the Voronoi diagram data structure, overwriting the entries of the deleted vertices.

9. Repeat Steps 2–8 for the next point.

5.3 Generation of the viscous layer

In higher Reynolds number flow, the subdivision of viscous layer is required to resolve phenomena. In the shape optimization, the structured mesh on viscous layer is also effective to obtain optimized shape stably. In this research, the boundary layer elements are introduced.
In two dimensions, triangulation of viscous layer is performed in very simple way as shown in figure 2. In another way, Delaunay tetrahedrization can be applied. The compatibility can be kept in Delaunay tetrahedrization. However, the Delaunay tetrahedrization in boundary layer also has a problem. The example is shown in figure 3. In the figure 3, some edges exist across the boundary layer. This situation is undesirable as boundary layer elements.

In three dimensions, tetrahedron can be made in the way as shown in figure 4. However, this procedure is not able to make element mesh. It is a way just to make tetrahedra. Incompatibility of adjacent tetrahedra occurs in the tetrahedrization process. Tetrahedrization keeping the compatibility should be complicated task.
Therefore, in this section, the scheme of generating boundary layer elements with keeping compatibility is proposed.

5.3.1 Picking Up method

Authors call this scheme 'Picking Up method'. Viscous surfaces are generated by following algorithm.

1. Generate triangular surface-elements and make the list of the surface-elements L_{surf}.

2. Calculate the unit normal vector at each nodal point on the boundary (See figure 5).

3. Select a node P, then generate new node Q. Q is placed in direction of normal vector form node P (See figure 6).

4. Search surface-elements S_{adj} which are adjacent to node P, from list L_{surf} (See figure 6).

5. Generate new tetrahedral elements connecting surface-elements S_{adj} and node Q(See figure 6.1, 6.2).

6. Remove surface-elements S_{adj} from list and add new surface-elements, which adjacent to node Q(See figure 6.3).

7. Loop from 2. to 6. over the number of nodes on boundary surface(See figure 7.3).

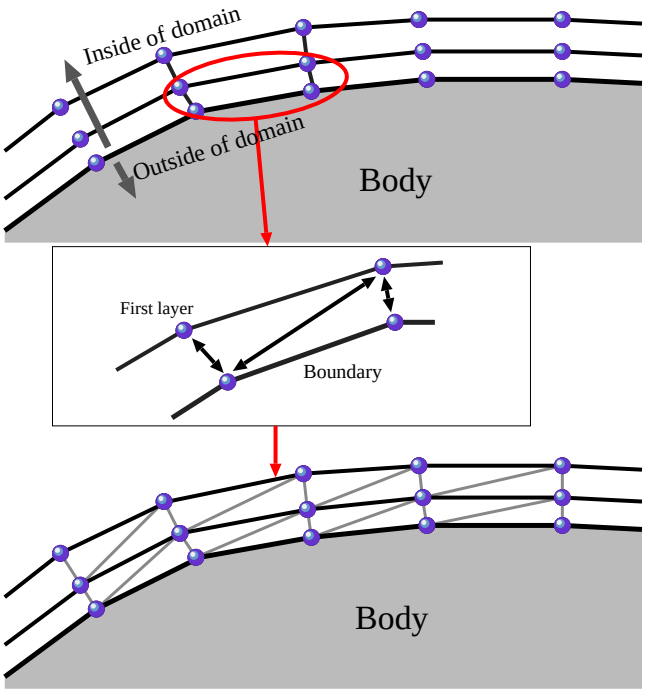

Figure 2: Triangulation between layers

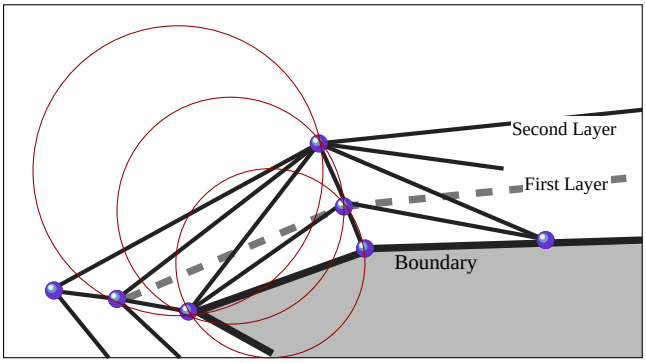

Figure 3: Viscous layer destroyed by Delaunay triangulation

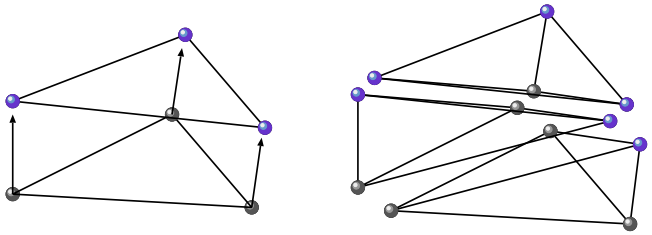

Figure 4: Tetrahedrization of prism

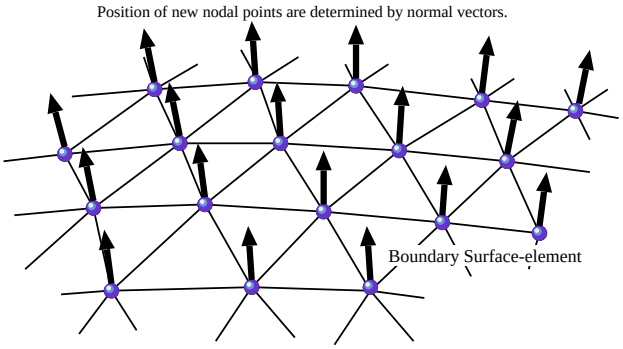

Figure 5: Normal vector at a nodal point on the boundary

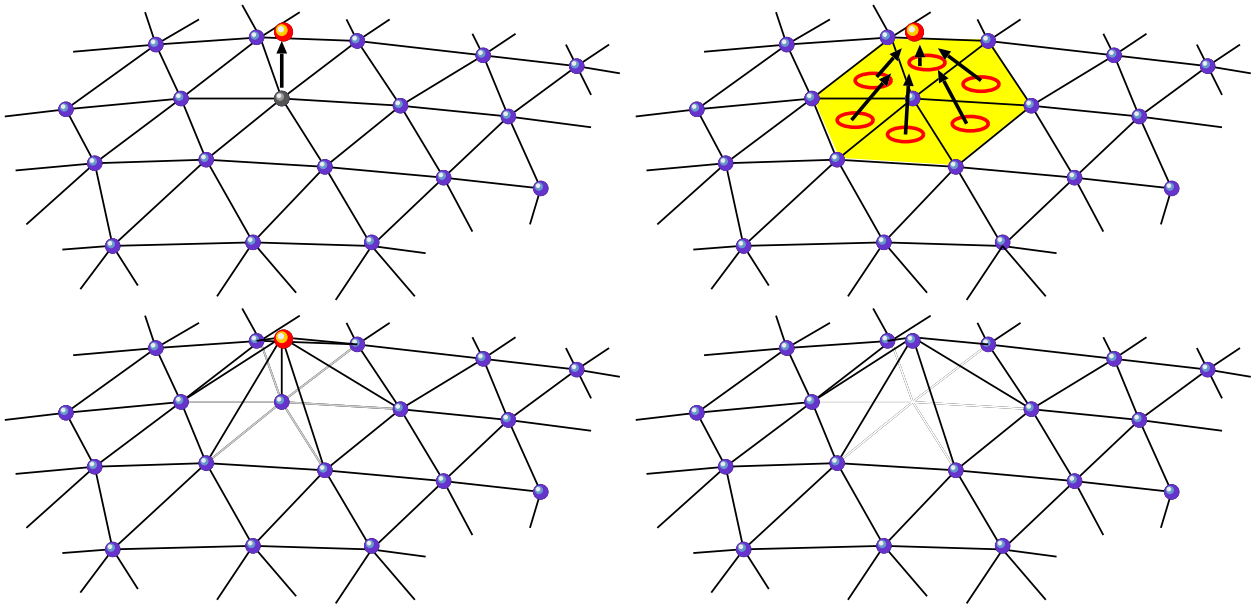

Figure 6: Generation of new elements: The first nodal point.

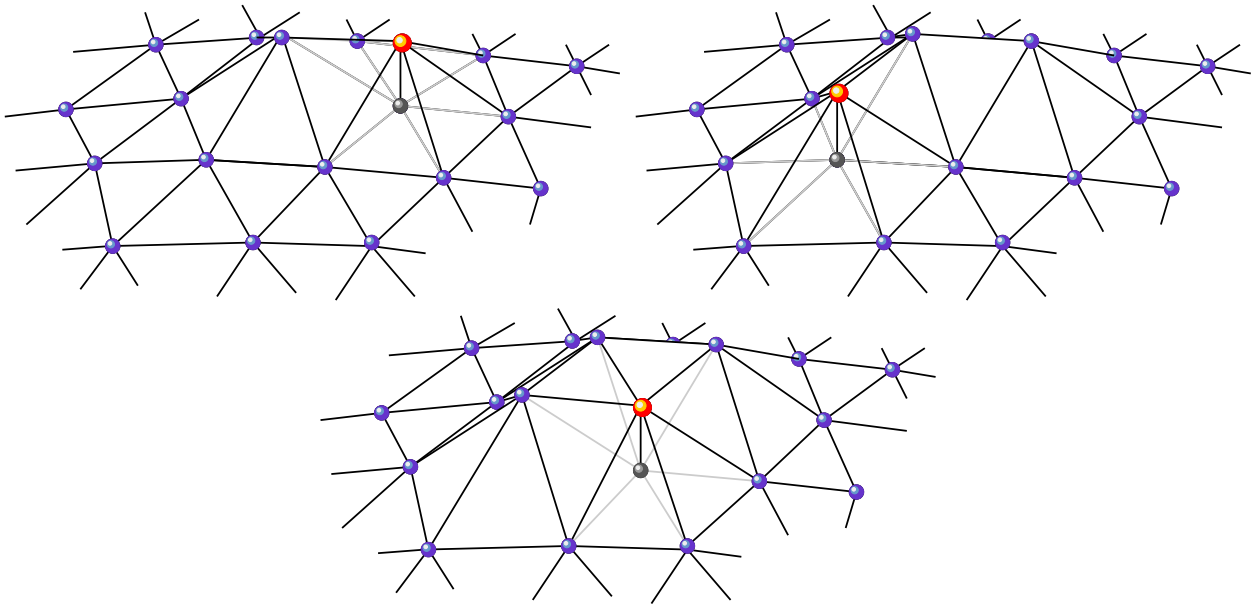

Figure 7: Generation of new elements: From the second to the fourth.

5.3.2 Algorithm of re-construction of finite element mesh with viscous layer

Algorithm of re-construction of finite element mesh with viscous layer is shown in figure 8. The figure shows two dimensional case, but the algorithm is also available to three dimensions. In the figure, "Shell mesh" means the finite element mesh which is constructed from nodal points on outer boundary.

First of all, two data are required. The first is the shell mesh, which constructed form only nodal points on outer boundary. The second is the profile of body which consists of nodal points. Then, finite element is re-constructed following algorithm.

1. The profile of the body is deformed according to the result of shape optimization;
2. The viscous layer is constructed around the body;
3. The nodal points on outer viscous layer is inserted into the shell mesh. Then Delaunay tetrahedrization is carried out;
4. Refinement of the finite element mesh is performed;
5. Finally, whole-domain mesh and viscous layer elements are combined.

6 NUMERICAL STUDY

As a numerical study, the drag force minimization problems are treated. In case that a body is located in the incompressible viscous flow, it is the purpose of the present paper to identify a shape that the drag force applied to the body is minimized.

6.1 Three dimensional Navier–Stokes flow

The objective value of drag force $\hat{F}_1$ is set to 0.0. The weighting parameter q_1, q_2 and q_3 are set to 1.0, 0.0, 0.0, respectively.

Figs. 9, 10 and 11 show the domain used in the computation and the finite element mesh. The total number of nodes and elements, which change in each iteration, are about 5,000 and 27,000 respectively. The Reynolds number is set to 1.0.

Figure 12 shows mesh shape of numerical optimal shape. Figure 13 shows convergent history of performance function and time-averaged drag force. The drag force in the case of final shape was reduced by about 4%. Figure 14 shows comparison between the initial shape and the result by the presented method. The figures **??** and **??** shows the section of the finite element mesh of the initial domain and the final domain, respectively. In both picture, it can be confirmed that the body is surrounded by structured mesh. The proposed mesh generation scheme works correctly.

Figure 17 is drag minimizing profile in the Stokes flow provided by O. Pironneau(1973). Pironneau obtained the shape by steepest descent method. In his shape optimization, the initial shape is the minimum drag ellipsoid revolution.

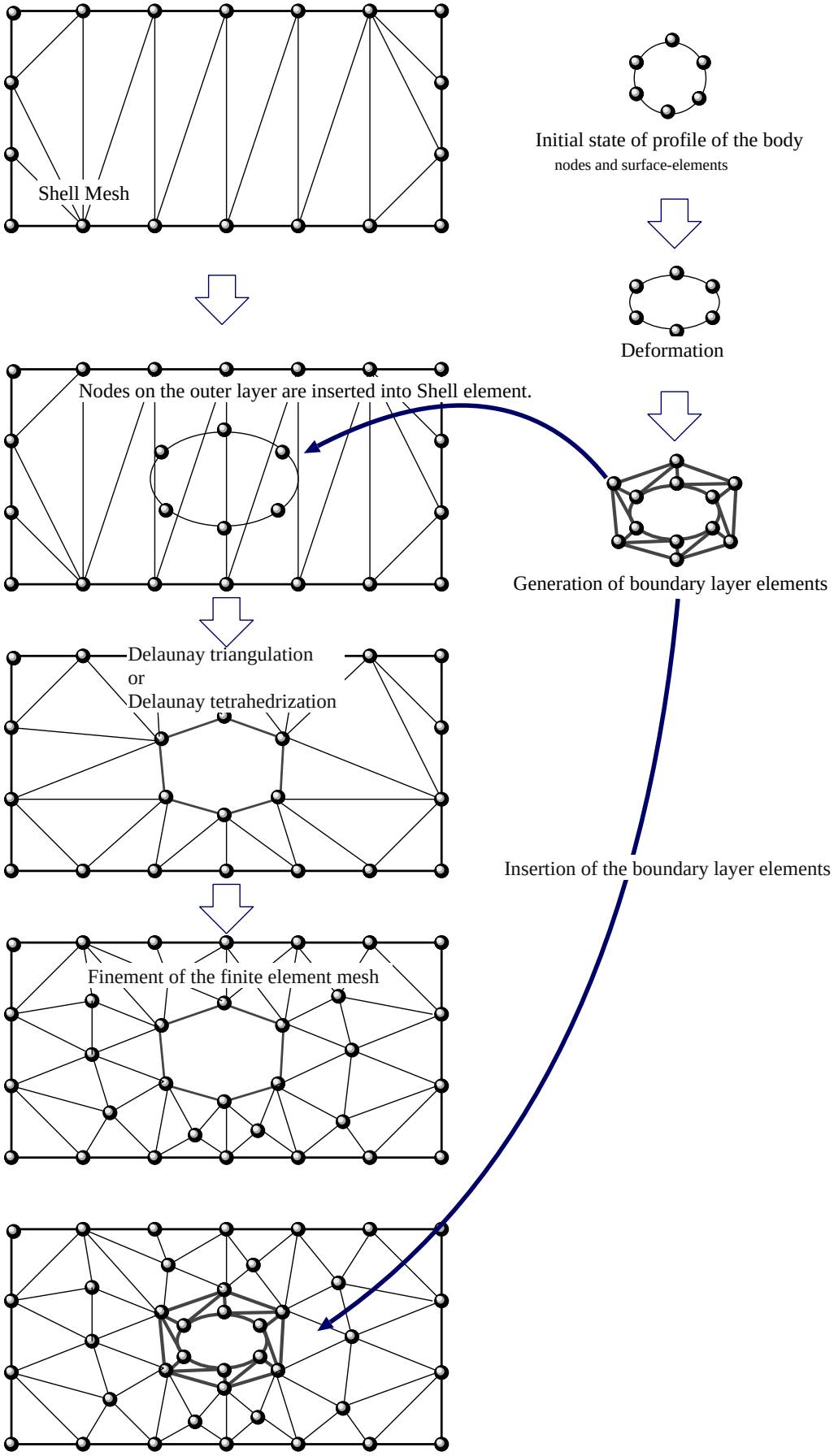

Figure 8: Finite element mesh–reconstruction algorithm

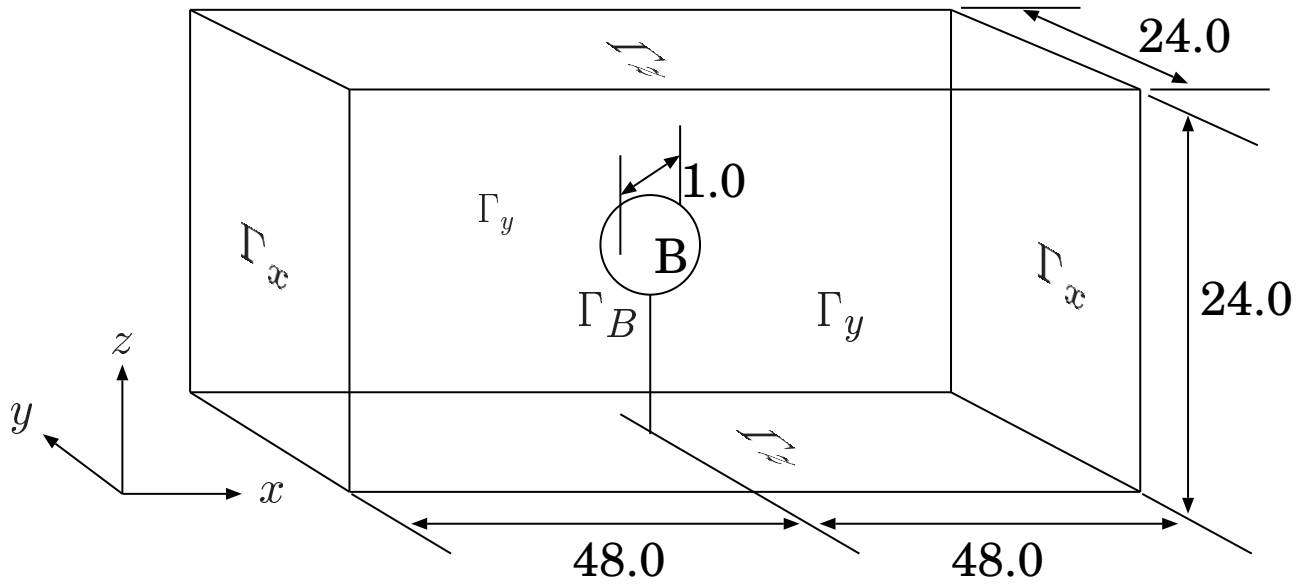

Figure 9: Domain used in the computation

Comparison between obtained shape and the shape by O. Pironneau is shown in 18. The obtained shape is not Pironneau's shape. However, the obtained shape is coincide with minimum drag ellipsoid revolution.

CONCLUSION

The shape optimization with three-dimensional re-meshing is carried out. Three-dimensional Delaunay triangulation is integrated to the shape optimization. The algorithm of boundary layer generation is newly introduced in this research. Re-meshing is performed correctly in the optimization process. The optimal shapes in case that the volume is constant to keep the initial volume are obtained by the formulation of shape optimization using the optimal control theory in Navier-Stokes flows. The gradient obtained by the first variation is directly applied to the shape optimization problem. It is confirmed that the obtained shape is quite near the result obtained by Pironneau, which is known as the minimum drag force shape. This result shows this formulation is adaptable to compute several drag force minimizing problem in the fluid flow.

REFERENCES

Hughes, T.J.R., Franca, L.P. and Balestra, M. (1986). "A new finite element formulation for computational fluid dynamics: V. Circumventing the Babuska-Brezzi condition: A stable Petrov-Galerkin formulation of the Stokes problem accommodating equal order interpolation", Comp. Methods. Appl. Mech. Eng. Vol. 59, pp. 85–99.

Maruoka, A. and Kawahara, M. (1998). "Optimal control in Navier-Stokes equation", Int. J. Comp. Fluid Dyn., Vol. 9, pp. 313–322.

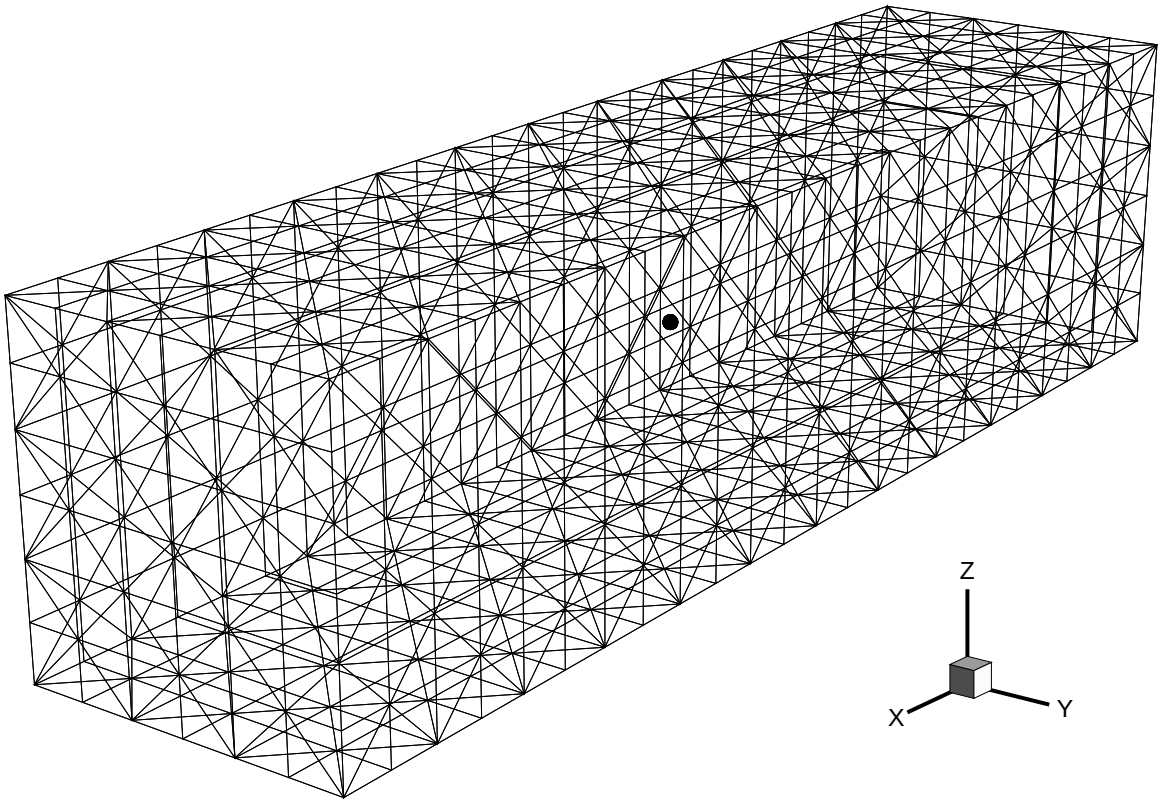

Figure 10: Initial finite element mesh

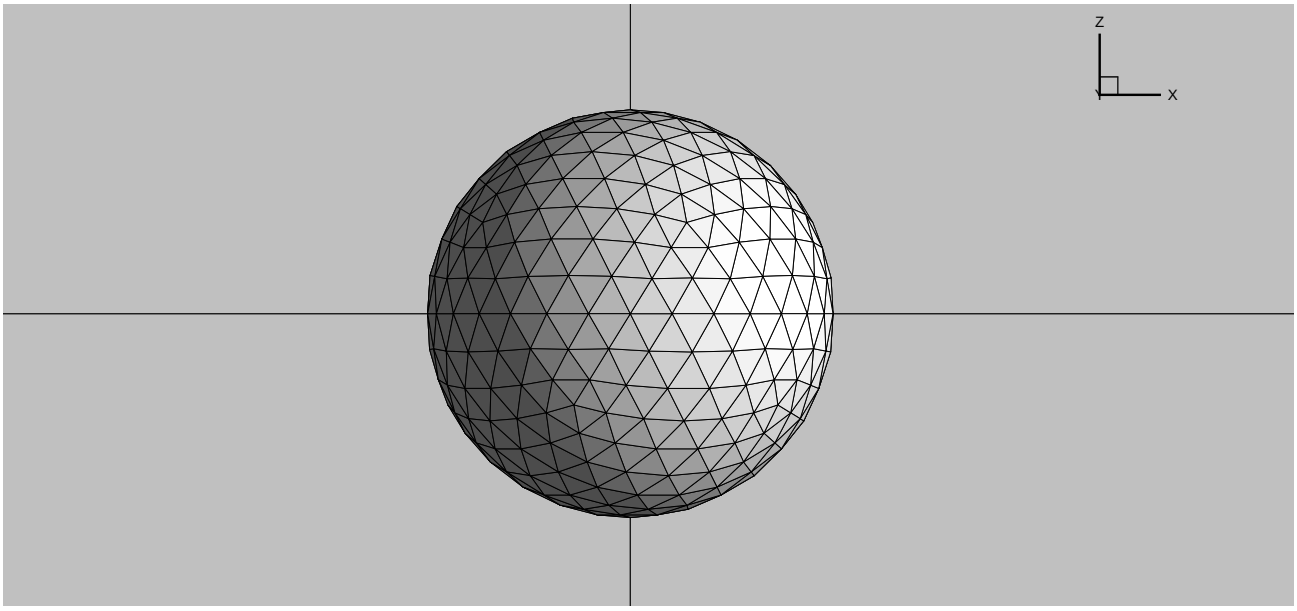

Figure 11: Initial shape

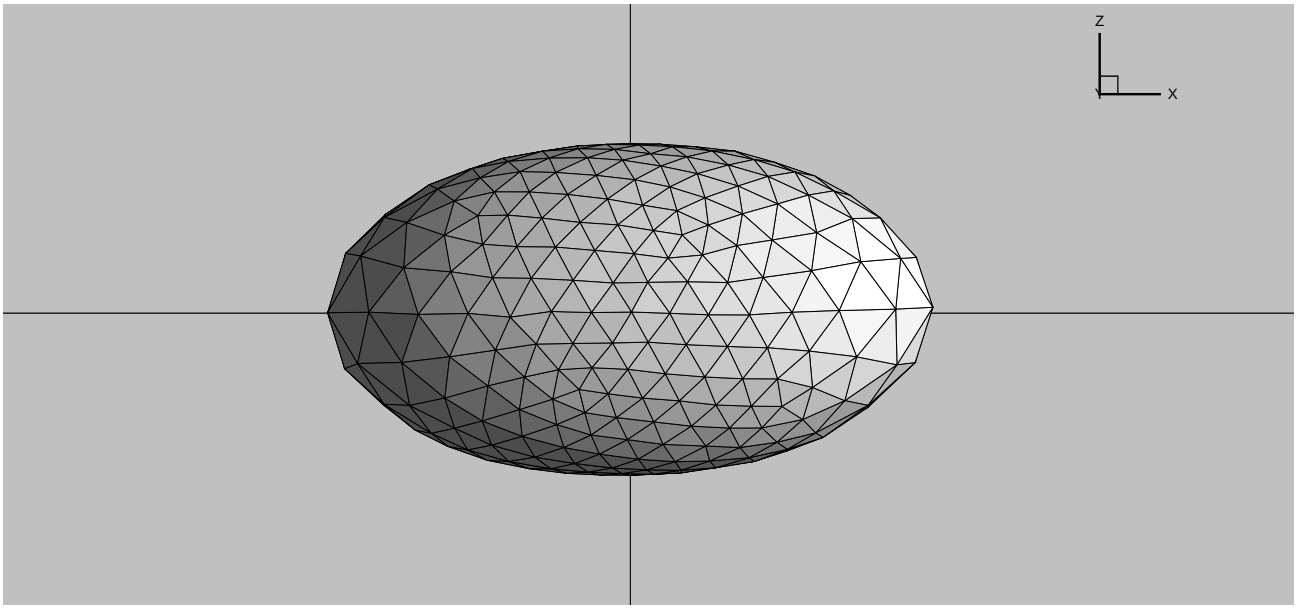

Figure 12: Obtained shape

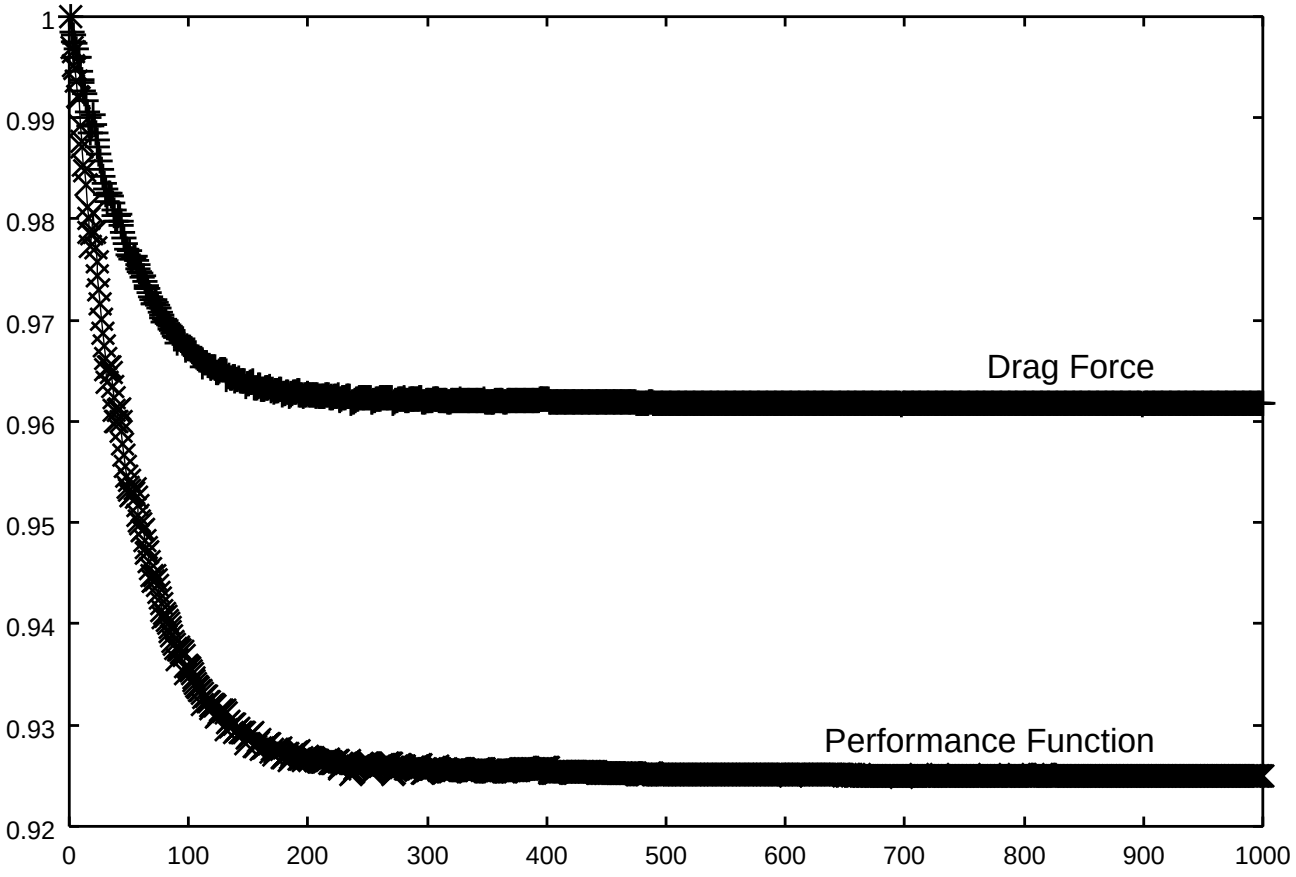

Figure 13: History of performance function J and time-averaged drag force.

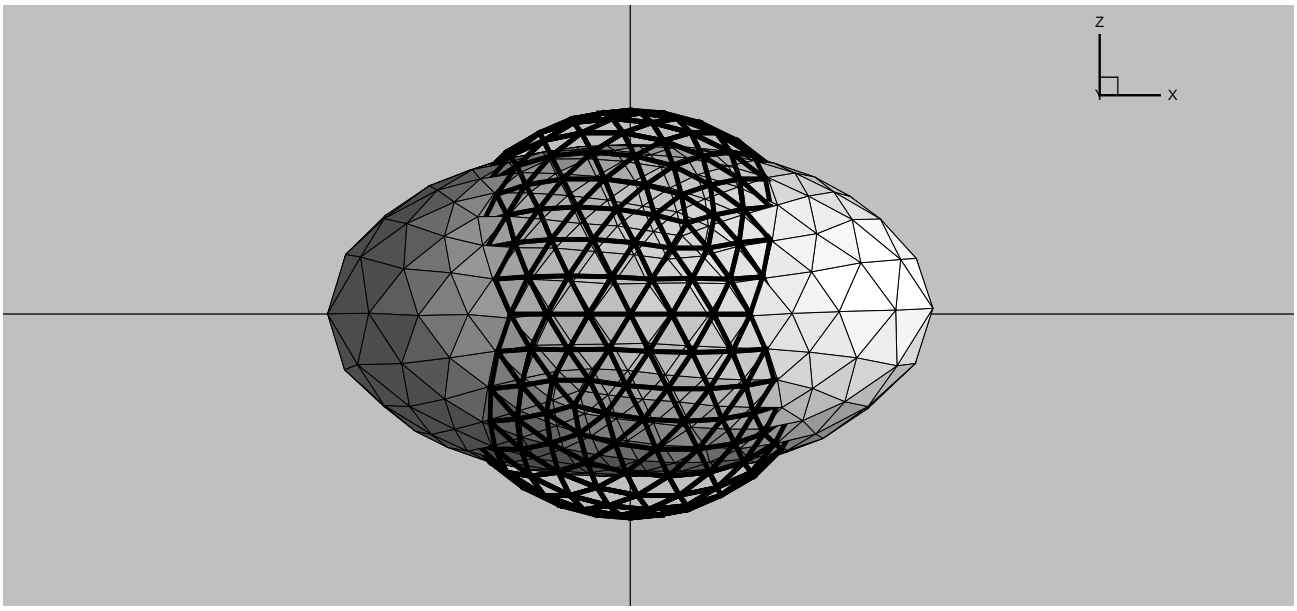

Figure 14: Comparison of the shape

Matsumoto, J., Umetsu, U. and Kawahara, M. (1999). "Incompressible viscous flow analysis and adaptive finite element method using linear bubble function", Journal of Applied Mechanics, Vol. 2, pp. 223–232.

Matsumoto, J. and Kawahara, M. (2000). "Stable shape identification for fluid-structure interaction problem using MINI element", Journal of Applied Mechanics, Vol. 3, pp. 263–274.

Ogawa, Y. and Kawahara, M. (2003). "Shape optimization a body located in incompressible viscous flow based on optimal control theory", Int. J. Comp. Fluid Dyn, Vol. 17, No. 4, pp. 243–251.

Pironneau, O. (1973). "On optimum profiles in Stokes flow", J. Fluid Mech, Vol. 59, No.1, pp. 117–128.

Pironneau, O. (1974). "On optimum design in fluid mechanics", J. Fluid Mech, Vol. 64, No.1, pp. 97–110.

Bowyer, A. (1981). "Computing Dirichlet tessellations", The Comput. J., Vol. 24, pp. 162–166.

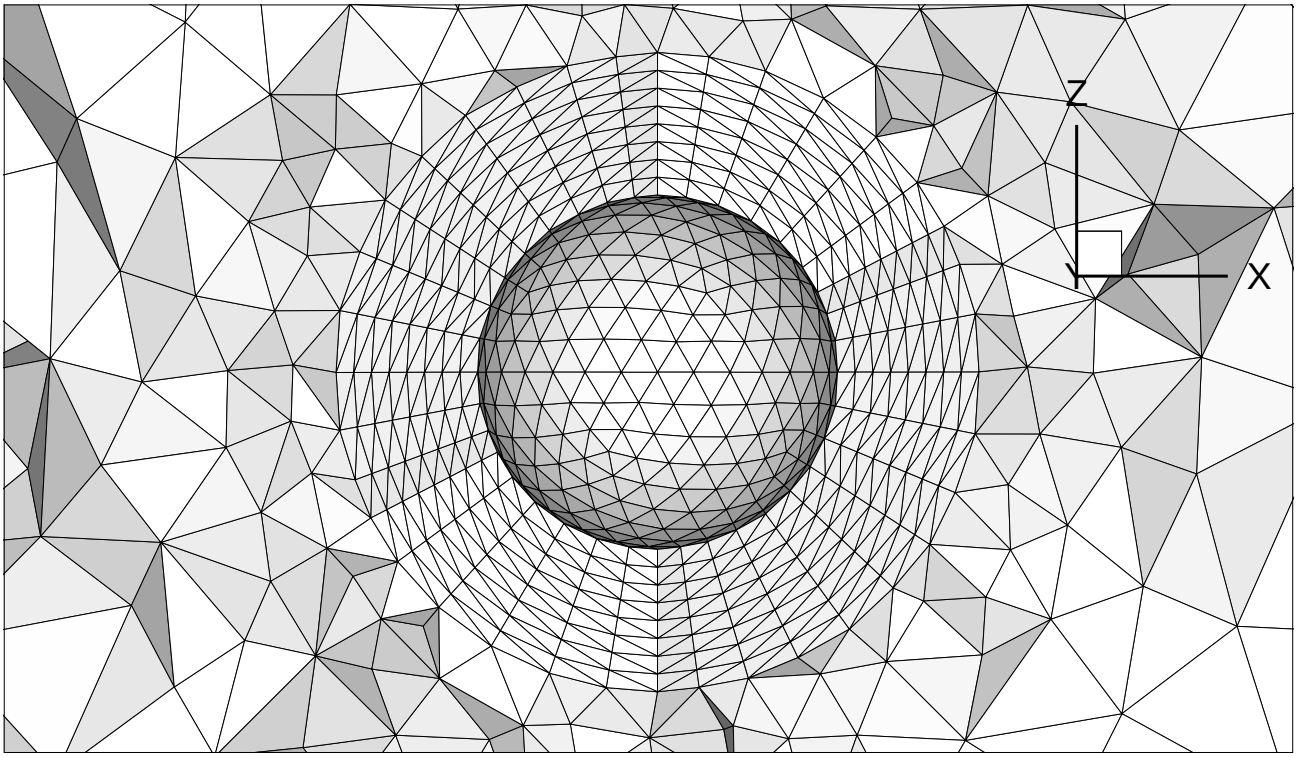

Figure 15: A Section of initial finite element mesh

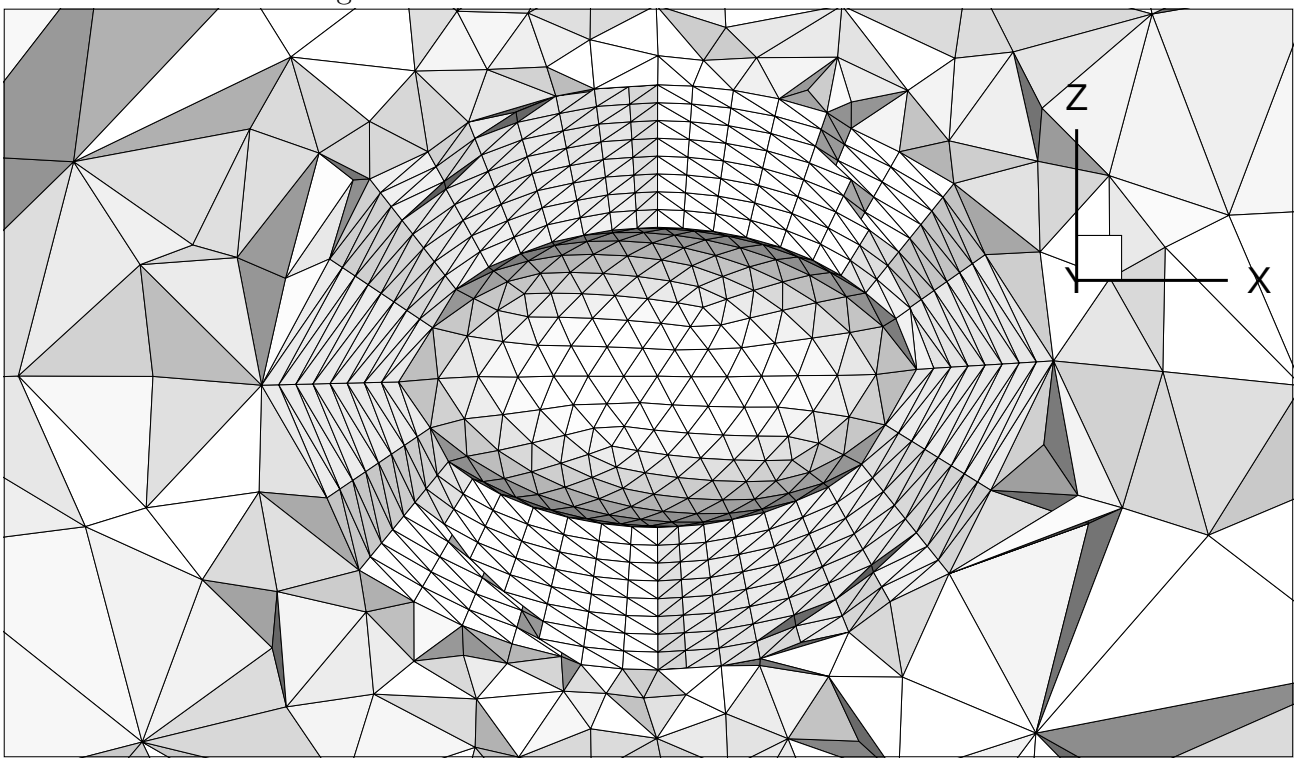

Figure 16: A Section of final finite element mesh

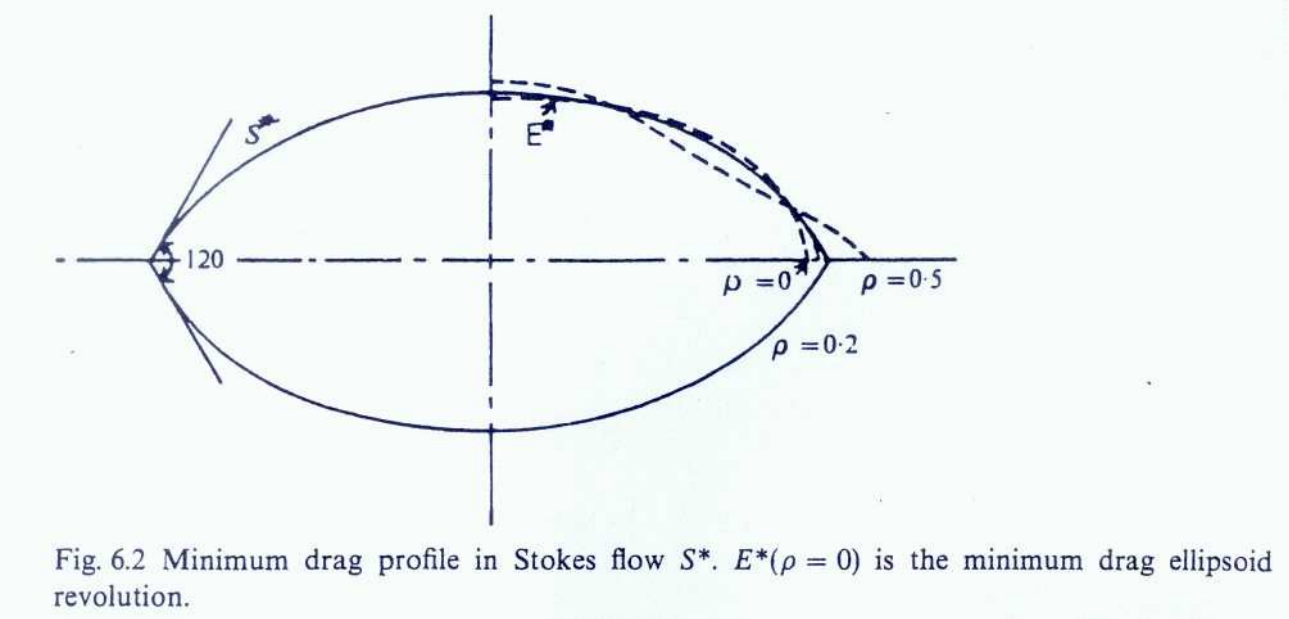

Fig. 6.2 Minimum drag profile in Stokes flow S^*. $E^*(\rho = 0)$ is the minimum drag ellipsoid revolution.

Figure 17: O.Pironneau's minimum drag shape

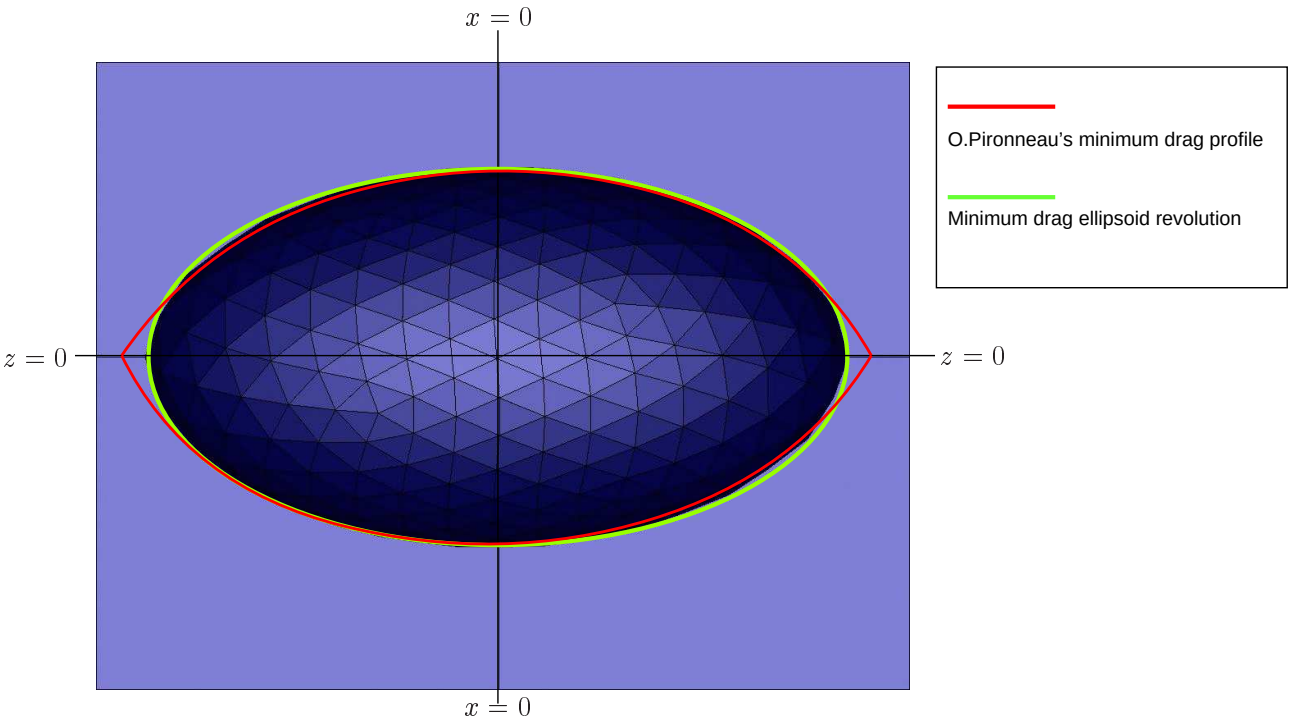

Figure 18: Comparison between obtained shape and Pironneau's shape